Noise properties and ac conductance of mesoscopic diffusive conductors with screening

Y. Naveh, D. V. Averin, and K. K. Likharev
Department of Physics, State University of New York, Stony Brook, New York 11794-3800
(Received 16 January 1998; revised manuscript received 11 August 1998)

A theory of nonequilibrium (''shot'') noise and high-frequency conductance in diffusive mesoscopic conductors with screening is presented. Detailed results are obtained for two simple geometries, for both large and short electron-electron scattering length l_{ee}, at frequencies of the order of the inverse Thouless time $1/\tau_T$. The conductance and the noise are found to exhibit significant frequency dependence. For $L \ll l_{ee}$, the high-frequency ($\omega\tau_T \gg 1$) shot-noise spectral density $S_I(\omega)$ approaches a finite value between $2eI/3$ and $2eI$, depending on the screening properties of the system, with temperature corrections to $S_I(\omega)$ being *linear* in T. However, when $L \gg l_{ee}$, $S_I(\omega)$ grows as $\omega^{1/4}$ (at $T=0$), is not upper-bound by $2eI$, and has a temperature-dependent component *quadratic* in T. As a result, measurements of $S_I(\omega,T)$ can be utilized as a probe of the strength of electron-electron scattering. [S0163-1829(98)05047-4]

I. INTRODUCTION

Significant attention has recently been focused on the dynamic electronic properties of mesoscopic systems. These properties include the ac conductance which gives the mean current response to applied ac voltage, and the noise, i.e., the deviations of the current from its average value. Due to the fluctuation-dissipation theorem, equilibrium Johnson-Nyquist noise, as measured in the external leads, does not convey any additional information to that obtained from the ac conductance. This is not the case for nonequilibrium (''shot'') noise. Here, the current fluctuations are dependent upon the nonequilibrium distribution function, as well as on electron-electron correlations. Moreover, the shot noise may be interpreted as an indication that the transport mechanism through the structure involves discrete transfer of charge, as opposed to the continuous charge transfer that takes place in macroscopic conductors.[1]

Earlier, shot noise in diffusive conductors was calculated in the zero-frequency limit,[2–6] with the conclusion that the low-frequency spectral density equals 1/3 of the classical Schottky value $2eI$, where I is the average (dc) current in the system. This result was obtained in two very different theoretical frameworks, namely in a quantum-mechanical transmission approach[2] which is generally based on the quantum coherence of the different electron states, and in a semiclassical approach,[3] in which quantum coherence is neglected, and the only effects on the noise are due to the single-particle nonequilibrium distribution function of the electrons. We believe that this surprising agreement between the two theories was adequately explained[7] by showing that the main ingredient in the quantum transmission approach, the bimodal distribution of transmission coefficients, is the only distribution compatible with Ohm's law, and thus can be asserted by semiclassical considerations alone.[8] The 1/3 suppression result is strictly valid only in a noninteracting electron picture. The electron-electron interaction slightly increases the zero-frequency noise value, which reaches $(\sqrt{3}/2)eI$ in the limit when the electrons are locally thermalized.[9,10]

One of the most important characteristics of classical shot noise is that it is white up to very high frequencies. In ballistic structures the noise is reduced only at frequencies of the order of the inverse time of flight of the electron across the device.[11] In diffusive conductors, there are at least three *a priori* candidates to the analog of this time constant: the elastic scattering time τ, the (much larger) ''Thouless'' time τ_T of electron diffusion through the sample, and the Maxwell relaxation time $\epsilon/4\pi\sigma$. In addition, quantum effects also may be manifested by a frequency-dependent noise spectrum, increasing the noise at $\omega > eV/\hbar$, where V is the applied voltage.[12] Recently we have shown[13] that even at high voltage, $eV \gg \hbar/\tau_T$, where quantum effects are negligible, the shot noise in diffusive structures may exhibit considerable frequency dependence at frequencies as low as $1/\tau_T$.[14] In that work, however, only the zero-temperature case was considered and the ac conductance and effects of electron-electron interaction were not explored.

The issue of high-frequency noise cannot be separated from that of the ac conductance at the same frequency. Previous works studied the ac conductance in diffusive structures with ring[15–18] or linear[19–21] geometries. In the first case, noninteracting electrons were considered, and the frequency dependence of the ac conductance was found to be similar to the Drude dependence,[16,17] i.e., appreciable only at $\omega \sim 1/\tau$. However, usual conductors (with electrodes) cannot be considered separately from their electrodynamic environment. For such conductors general expressions for the conductivity were obtained to linear order in the frequency.[19–21] Under the assumption of absolute local electroneutrality, it was found that this linear correction (the ''emittance'') vanishes and the conductance is again independent of the frequency up to $\omega \sim 1/\tau$.[21] Here we are interested in the case where the conductor's length L or its thickness t are comparable to the screening length λ, so local charge neutrality may no longer be retained. While we confirm the previous results[21] for $L,t \gg \lambda$, we show that observable deviations from them may appear already at $L/\lambda \sim 10$ or $t/\lambda \sim 10$.

A vast amount of research has been dedicated to the effects of weak localization on the dc conductance of mesoscopic diffusive conductors.[22] Its effect on the ac conductance[23,24] and the high-temperature noise ($T > eV$)

(Ref. 25) led to corrections to these quantities which are of the order of the quantum unit of conductance e^2/h (times some characteristic energy in the case of noise). These corrections will be neglected in this work, since we will consider the case of conductance much higher than e^2/h, so that deviations of the high-frequency conductance and the noise from their zero-frequency values are much larger than the weak localization corrections.

In the present work the noise properties and the ac conductance of diffusive conductors much shorter than the electron-phonon mean free path are calculated at frequencies comparable to $1/\tau_T$ or $4\pi\sigma/\epsilon$, with account of screening.[26] Throughout the work we assume that the electrons form a degenerate gas with Fermi wavelength λ_F much smaller than the elastic mean free path l, while $l \ll L, \lambda$. This allows us to use the Boltzmann-Langevin approach introduced by Kogan and Shulman[27] (see also Ref. 28), and study both the ac conductance and the noise in a unified way. In Sec. II we analyze the Boltzmann-Langevin equation in a nonuniform structure, obtain the boundary conditions for the distribution function at the conductor-electrode interface, and derive a ''drift-diffusion-Langevin'' equation for the current. In Sec. III we apply this equation to two specific models of diffusive conductors (a ''sandwich'' and a conductor over a ground plane). In Sec. IV the kernels, which describe the response of the system to external voltage, and to the random Langevin sources, are found. Using these response functions we calculate the conductance and thermal noise (Sec. V), and the nonequilibrium shot noise (Sec. VI). Section VII presents a discussion of the results and conclusions.

II. BOLTZMANN-LANGEVIN-POISSON THEORY

In order to describe both the conductor and electrodes, we need self-consistent equations for the current in a system which may be substantially nonuniform on a scale $\Delta r \gg l$. In the diffusion approximation the electron distribution function can be written as

$$f = f(\varepsilon, \cos\,\theta, \mathbf{r}, t) = f_s(\varepsilon, \mathbf{r}, t) + f_a(\varepsilon, \mathbf{r}, t)\cos\,\theta, \quad (2.1)$$

where $|f_a| \sim l/L \ll 1$ and ε is the total electron energy,

$$\varepsilon = \varepsilon_{\mathbf{k}} + \varepsilon_c(\mathbf{r}) - e\Phi(\mathbf{r}, t) \equiv \varepsilon_{\mathbf{k}} + U(\mathbf{r}, t). \quad (2.2)$$

Here $\varepsilon_{\mathbf{k}}$ is the kinetic energy of an electron with momentum $\mathbf{k}$ while $\varepsilon_c(\mathbf{r})$ is the equilibrium local conduction-band edge, which includes possible band-bending due to mismatch in the local Fermi energies in the nonuniform conductor, and hence describes the equilibrium (''built-in'') electric field $\mathbf{E}_0 = -\nabla\varepsilon_c/e$. θ is the angle between $\mathbf{k}$ and the direction of the current, and $\Phi(\mathbf{r}, t)$ is the time-dependent electric potential, so that $U(\mathbf{r}, t)$ is the total instantaneous potential energy of the electrons. In the above variables, the velocity of the particle is both position- and time-dependent, $v = v(\varepsilon, \mathbf{r}, t)$, and the Boltzmann equation within the usual relaxation-time approximation looks like

$$\frac{\partial f}{\partial t} + \frac{\partial f}{\partial \varepsilon}\frac{\partial U}{\partial t} - \frac{\partial f}{\partial \cos\,\theta}\frac{\partial \cos\,\theta}{\partial \mathbf{k}} \cdot \nabla U + \nabla f \cdot \mathbf{v} + \frac{f_a \cos\,\theta}{\tau} = 0, \quad (2.3)$$

where $\tau = \tau(\mathbf{r})$ is the local elastic relaxation time. Note that in the diffusion approximation the term proportional to ∇U is usually neglected, since it is of the order of f_a^2. However, in our case this term may be linear in f_a, because ∇U has the component $\nabla\varepsilon_c$ even in the absence of current.

As usual,[29] we proceed by separating Eq. (2.3) into its symmetric and antisymmetric parts [see Eq. (2.1)] and in the first order in f_a we get

$$\frac{\partial f_s}{\partial t} + \frac{\partial f_s}{\partial \varepsilon}\frac{\partial U}{\partial t} - f_a \frac{\partial \cos\,\theta}{\partial \mathbf{k}} \cdot \nabla U + \nabla f_a \cdot \mathbf{v} \cos\,\theta = 0, \quad (2.4a)$$

$$\left(\frac{\partial}{\partial t} + \frac{1}{\tau}\right) f_a \cos\,\theta + \nabla f_s \cdot \mathbf{v} = 0. \quad (2.4b)$$

In this work we are interested only in the case of frequencies much smaller than $1/\tau$. In this case Eqs. (2.4) may be combined to give

$$\frac{\partial f_s}{\partial t} + \frac{\partial f_s}{\partial \varepsilon}\frac{\partial U}{\partial t} + \nabla f_s \cdot \frac{\mathbf{v}\tau}{\cos\,\theta}\frac{\partial \cos\,\theta}{\partial \mathbf{k}} \cdot \nabla U - \nabla(\nabla f_s \cdot \mathbf{v}\tau) \cdot \mathbf{v} = 0. \quad (2.5)$$

Integration of this equation over the directions of $\mathbf{k}$ gives

$$\frac{\varepsilon_{\mathbf{k}} l}{D}\frac{\partial f_s}{\partial t} - \nabla \cdot [\varepsilon_{\mathbf{k}} l \nabla f_s] - \frac{3}{2} l \nabla_\perp f_s \cdot \nabla_\perp U = 0 \quad (2.6)$$

with $D = D(\mathbf{r}) = l(\mathbf{r})v_F(\mathbf{r})/3$ and $l = l(\mathbf{r}) = \tau(\mathbf{r})v_F(\mathbf{r})$, v_F being the Fermi velocity. $\nabla_\perp$ denotes differentiation in the plane perpendicular to the current direction x. Equation (2.6) is a generalization of the regular diffusion equation for the distribution function in the case when the potential or the mean free path change substantially in space.

The random nature of the scattering in the conductor may be described[27,28] by a stochastic source term $J^s(\mathbf{r}, \mathbf{k}, t)$, with zero average, added to the right-hand side of Eq. (2.3). Its correlation function was found by Kogan and Shul'man[27] assuming Poisson statistics of the scattering events, and taking into account the Fermi correlations of the electrons. For the case of strong isotropic impurity scattering ($l \ll L$) the result reads

$$\langle J_a^s(\mathbf{r}, \varepsilon, t) J_a^s(\mathbf{r}', \varepsilon', t') \rangle = \frac{6\,\delta(\mathbf{r}-\mathbf{r}')\,\delta(\varepsilon-\varepsilon')\,\delta(t-t')}{\tau(\mathbf{r})\mathcal{N}(\mathbf{r})} \times \overline{f}_s(\varepsilon, \mathbf{r})[1 - \overline{f}_s(\varepsilon, \mathbf{r})], \quad (2.7)$$

where J_a^s is the antisymmetric component of J^s, $\mathcal{N}(\mathbf{r})$ is the local density of states at the Fermi level (excluding the spin degeneracy), and $\overline{f}$ is the ensemble average of the distribution function.

Equations for the current can be obtained by including the source term J^s in Eqs. (2.4), and then integrating them over the electrons' momenta. It is convenient at this stage to change variables in Eqs. (2.4) from ε to $\varepsilon_{\mathbf{k}}$ by using Eq. (2.2). Integrating Eq. (2.4a) over $\mathbf{k}$, we get the continuity equation

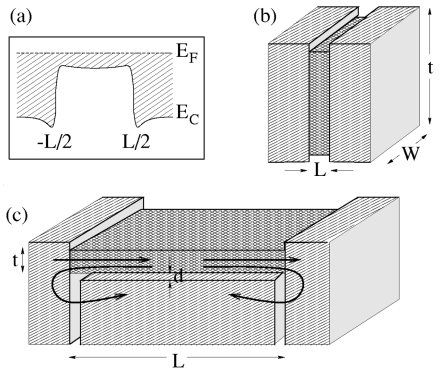

FIG. 1. Schematic description of the geometries studied. (a) The conduction band-edge profile in both models. (b) The sandwich model. (c) The ground-plane model.

$$\frac{\partial}{\partial t}\rho(\mathbf{r},t)+\boldsymbol{\nabla}\cdot\mathbf{j}(\mathbf{r},t)=0 \tag{2.8}$$

with $\mathbf{j}(\mathbf{r},t)$ the current density and $\rho(\mathbf{r},t)$ the excess electron density, i.e., the total charge density minus its equilibrium value $\rho_0(\mathbf{r})$ (which includes the possible charge transfer when two materials have been brought into contact). The Langevin term integrates out from this equation, as expected for particle-conserving scattering processes.

If, before integration over $\mathbf{k}$, we multiply Eq. (2.4b) (including the Langevin term) by $\mathbf{v}$, it yields

$$\begin{aligned}\mathbf{j}(\mathbf{r},t)=&-D(\mathbf{r})\boldsymbol{\nabla}[\rho_0(\mathbf{r})+\rho(\mathbf{r},t)]\\&+[\sigma(\mathbf{r})+\delta\sigma(\mathbf{r},t)][\mathbf{E}_0(\mathbf{r})+\mathbf{E}(\mathbf{r},t)]+\mathbf{j}^s(\mathbf{r},t)\end{aligned} \tag{2.9}$$

with $\sigma(\mathbf{r})=e\tau(\mathbf{r})\rho_0(\mathbf{r})/m(\mathbf{r})$ and $\delta\sigma(\mathbf{r},t)=e\tau(\mathbf{r})\rho(\mathbf{r},t)/m(\mathbf{r})$. Here $m(\mathbf{r})$ is the local effective mass (for simplicity, the parabolic and isotropic dispersion relation was assumed), and

$$\mathbf{j}^s(\mathbf{r},t)=e\tau(\mathbf{r})\sum_{\mathbf{k}}\mathbf{v}_{\mathbf{k}}J^s(\mathbf{r},\mathbf{k},t). \tag{2.10}$$

At equilibrium, and in the absence of external fluctuation sources, the current $\mathbf{j}(\mathbf{r},t)$ should vanish. Thus, the built-in electric field satisfies the equation

$$-D(\mathbf{r})\boldsymbol{\nabla}\rho_0(\mathbf{r})+\sigma(\mathbf{r})\mathbf{E}_0(\mathbf{r})=0 \tag{2.11}$$

which may be interpreted as the constancy of the electrochemical potential at $V=0$ and $j^s=0$.

The terms proportional to $\delta\sigma(\mathbf{r},t)$ in Eq. (2.9) are negligible if

$$e|\Phi_0(\mathbf{r})+\Phi(\mathbf{r},t)|\ll\varepsilon_F-\varepsilon_c(\mathbf{r}) \tag{2.12}$$

(where ε_F is the equilibrium Fermi energy [Fig. 1(a)]), i.e., if the band bending and the external potential are small compared to the local Fermi energy. Under the condition (2.12), Eq. (2.9), together with the constraint (2.11), yield the ''drift-diffusion-Langevin'' equation

$$\mathbf{j}(\mathbf{r},t)=\sigma(\mathbf{r})\mathbf{E}(\mathbf{r},t)-D(\mathbf{r})\boldsymbol{\nabla}\rho(\mathbf{r},t)+\mathbf{j}^s(\mathbf{r},t), \tag{2.13}$$

where the variables include both the deterministic and stochastic parts.

The correlation function of the current sources $\mathbf{j}^s$ in any direction α follows from Eqs. (2.7) and (2.10):

$$\langle j^s_\alpha(\mathbf{r},t)j^s_\alpha(\mathbf{r}',t')\rangle=\delta(\mathbf{r}-\mathbf{r}')\,\delta(t-t')\mathcal{S}(\mathbf{r}) \tag{2.14}$$

with the correlator

$$\mathcal{S}(\mathbf{r})=\frac{2}{3}e^2\tau(\mathbf{r})\mathcal{N}(\mathbf{r})v_F^2(\mathbf{r})\int_0^\infty d\varepsilon\,\overline{f}_s(\varepsilon,\mathbf{r})[1-\overline{f}_s(\varepsilon,\mathbf{r})]. \tag{2.15}$$

Now let us consider a system in which a homogeneous conductor connects two homogeneous electrodes with interfaces at $\pm L/2$, with the only source of inhomogeneity being the band bending due to charge transfer between the materials [Fig. 1(a)]. Let the interfaces be normal to the x axis and much sharper than the screening lengths λ,λ_e in the conductor and the electrodes, respectively. We define the interface regions to be the regions of width 2δ around $\pm L/2$, with $l\ll\delta\ll\lambda,\lambda_e,L$. A major assumption of this work is that the voltage in the system drops entirely in the bulk of the conductor, i.e., the resistances of the electrodes and the electrode-conductor interfaces are small compared to that of the conductor. This is the natural situation when the electrodes are of high conductivity and when the interfaces are smooth on the scale of λ_F, so no reflections of electrons occur at the interfaces.

Let us consider, for example, the interface at $L/2$ and define $f_s^c=f_s(L/2-\delta)$ and $f_s^e=f_s(L/2+\delta)$. Since the voltage drop in the electrode is negligible, f_s^e is just the equilibrium Fermi-Dirac distribution

$$f_s^e=f_0(\varepsilon+eV/2)=\frac{1}{1+\exp\left(\dfrac{\varepsilon+eV/2-\mu}{T}\right)}, \tag{2.16}$$

where the chemical potential μ is defined as the average of the chemical potentials in the two electrodes. Moreover, the fact that there is no voltage drop across the interface region implies that f_s^c is also given by Eq. (2.16), $f_s^c=f_s^e$. Integrating this equation over the electron's momenta and using the relation $\mathcal{N}(\mathbf{r})=\epsilon/4\pi e^2\lambda^2(\mathbf{r})$ leads to the first boundary condition at the electrode-conductor interface,[30]

$$\lambda^2\rho^c=\lambda_e^2\rho^e \tag{2.17}$$

with $\rho^c\equiv\rho(L/2-\delta)$ and $\rho^e\equiv\rho(L/2+\delta)$.

The second boundary condition is the continuity of the current across the interface,

$$j_x^c=j_x^e \tag{2.18}$$

with j_x^c,j_x^e the transverse current densities at $L/2-\delta$, $L/2+\delta$, respectively.[31]

If complemented with the Poisson equation

$$\boldsymbol{\nabla}\cdot\mathbf{E}(\mathbf{r},t)=\frac{4\pi}{\epsilon(\mathbf{r})}\rho(\mathbf{r},t), \tag{2.19}$$

where $\epsilon(\mathbf{r})$ is the dielectric constant, Eqs. (2.8) and (2.13)–(2.19) form a closed system which is the basis for our calculations.

III. MODELS

A. The sandwich model

We study two analytically solvable models which differ in their assumed sample geometry, and hence in electrostatics.[13] In our first, ''sandwich'' model, which is schematically shown in Fig. 1(b), a short conductor of length $L \ll t$ is sandwiched between two wide electrodes (t is the smallest transverse dimension of the conductor). Defining the quantities $\Phi_\omega(x)$, $q_\omega(x)$, $E_\omega(x)$, $I_\omega(x)$, and $I^s_\omega(x)$ as integrals over the sample's cross section of the temporal Fourier components of $\Phi(\mathbf{r},t)$, $\rho(\mathbf{r},t)$, $E_x(\mathbf{r},t)$, $J_x(\mathbf{r},t)$, and $j^s_x(\mathbf{r},t)$, respectively, we get from Eqs. (2.8), (2.13), and (2.19),

$$-i\omega q_\omega(x)+\frac{dI_\omega(x)}{dx}=0, \tag{3.1}$$

$$I_\omega(x)=\sigma(x)E_\omega(x)-D(x)\frac{dq(x)}{dx}+I^s_\omega(x), \tag{3.2}$$

$$\frac{dE_\omega(x)}{dx}=\frac{4\pi}{\epsilon(x)}q_\omega(x). \tag{3.3}$$

[Deriving Eq. (3.3), we have neglected the transverse derivatives of $\mathbf{E}(\mathbf{r},t)$, since, by Gauss' theorem, they are proportional to the circumference of the cross section of the sample, while the derivative in the x direction is proportional to the cross-section area.]

Integration of Eqs. (3.1) and (3.3) provides a simple relation between the current and the electric field,

$$I_\omega(x)=\frac{i\omega\epsilon(x)}{4\pi}E_\omega(x)+I^e_\omega. \tag{3.4}$$

The integration constant I^e_ω has the physical sense of the current induced deep inside the electrodes (where $E_\omega=0$). It can be found from the condition that the current fluctuations do not affect the voltage V_ω applied to the structure:

$$\int_{-\infty}^{\infty}dx\,\frac{4\pi}{i\omega\epsilon(x)}[I^e_\omega-I_\omega(x)]=V_\omega. \tag{3.5}$$

Inserting Eqs. (3.1) and (3.4) in Eq. (3.2) we get the basic equation of this model,

$$\frac{d^2I_\omega(x)}{dx^2}-\kappa^2(x,\omega)I_\omega(x)=\frac{i\omega}{D(x)}I^s_\omega(x)-\frac{1}{\lambda^2(x)}I^e_\omega, \tag{3.6}$$

with

$$\kappa^2(x,\omega)=\frac{1}{\lambda^2(x)}-\frac{i\omega}{D(x)}, \tag{3.7}$$

and the static screening length is given by $\lambda(x)=[\epsilon(x)D(x)/4\pi\sigma(x)]^{1/2}$. Equation (3.6) is valid for both the conductor itself and the electrodes.

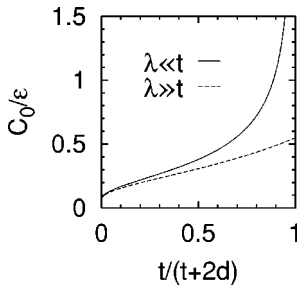

FIG. 2. The dependence of C_0 on $R/h=t/(t+2d)$ for a homogeneous cylindrical conductor close to a ground plane.

B. The ground-plane model

In the second (''ground plane'') model we consider a long and thin conductor close and parallel to a well-conducting ground plane, $L \gg t,d$, where t is the thickness of the conductor and d is its distance from the ground plane—see Fig. 1(c). The width of the conductor W (i.e., its second dimension, parallel to the ground plane) can be arbitrary. As we will show below, this geometry is more promising for experimental observation of some of the effects studied in this work.

In the same way as for the previous model, Eqs. (2.8) and (2.13) can be replaced with their 1D versions, i.e., Eqs. (3.1) and (3.2), respectively. The Poisson equation, however, leads to a different one-dimensional equation since in this model the gradient of the field in the x direction is much smaller than the transverse gradients. In this case, the linearity of the Poisson equation leads to a linear dependence of the potential on the local charge, both integrated over the conductor's cross section:

$$\Phi_\omega(x)=\frac{Aq_\omega(x)}{C_0}, \tag{3.8}$$

where A is the cross-sectional area and C_0 is the specific capacitance (per unit length).

For a homogeneous cylindrical conductor of radius $R=t/2$ and distance $h=t/2+d$ between its center and the ground plane, C_0 assumes the following limiting values: if the conductor is thick ($t \gg \lambda$),[32]

$$C_0=\frac{\epsilon_m}{2\cosh^{-1}(h/R)}\quad (R\gg\lambda), \tag{3.9}$$

with ϵ_m the dielectric constant of the medium between the conductor and the ground plane. In the opposite limit, the cylinder is uniformly charged. Taking for simplicity $\epsilon=\epsilon_m$, one finds

$$C_0=\frac{2\epsilon}{1+4\ln(h/R)+4I(h/R)}\simeq\frac{2\epsilon}{1+4\ln(2h/R)}\quad (R\ll\lambda), \tag{3.10}$$

with

$$I(b)\equiv\int_0^1 dx\,\ln\left(1+\sqrt{1-\frac{x}{4b^2}}\right). \tag{3.11}$$

The dependences of C_0 on the ratio R/h are shown in Fig. 2.

If the conductor is a uniform strip of width $W \gg d,t$, then

$$C_0=\frac{\epsilon_m W}{4\pi d} \quad (t\gg\lambda), \tag{3.12a}$$

$$C_0=\frac{\epsilon W}{4\pi(d+t/3)} \quad (t\ll\lambda). \tag{3.12b}$$

In the quantum limit, with only the first quantum level populated, C_0 may still be presented with Eq. (3.12b), though the thickness t must be replaced by an effective thickness $t_{\rm eff}$. For a square well potential with infinite barriers the effective thickness is

$$t_{\rm eff}=t\left(1+\frac{3}{4\pi^2}\right)\simeq 1.07t. \tag{3.13}$$

Combining Eq. (3.2) with Eq. (3.8) provides a diffusion-like relation between the current and the linear charge density,

$$I_\omega(x)=-D'\frac{dq_\omega(x)}{dx}+I^s(x), \tag{3.14}$$

with

$$D'=D+\frac{\sigma A}{C_0}. \tag{3.15}$$

With the help of Eq. (3.1) we once again get a simple equation for the current

$$\frac{d^2I_\omega(x)}{dx^2}-\overline{\kappa}^2(\omega)I_\omega(x)=-\overline{\kappa}^2(x,\omega)I^s_\omega(x) \tag{3.16}$$

with

$$\overline{\kappa}^2(\omega)=-\frac{i\omega}{D'}. \tag{3.17}$$

We now analyze the conditions under which Eq. (3.8) is valid. Expanding Eq. (3.16) in spatial harmonics we see that harmonics with wave number $k_x\gg|\overline{\kappa}|=\sqrt{\omega/D'}$ contribute negligibly to the current fluctuations I_ω. Thus, at frequencies $\omega\lesssim\overline{\tau_T}^{-1}\equiv D'/L^2\ll D'/d^2,D'/t^2$, we can consider only the wave numbers k_x which are much smaller than d^{-1},t^{-1}. For these harmonics, the transversal gradients of the electric field dominate in the Poisson equation, justifying Eq. (3.8) at that frequency range.

Equation (3.8) is not valid at distances comparable to d from the interface with the electrodes. Equation (3.16) should therefore be solved only inside the conductor, with boundary conditions at $\pm L'/2=\pm(L/2-\delta)$, where δ is now some distance for which $d\ll\delta\ll L,1/|\overline{\kappa}|$. To find these boundary conditions we write down Eq. (3.2) (which is valid even near the interface) in the form

$$I_\omega(x)=-\sigma\frac{d}{dx}\left[\Phi_\omega(x)+\frac{4\pi}{\epsilon}\lambda^2 q_\omega(x)\right]. \tag{3.18}$$

[The sources $I^s(x)$ in the small interface region may be neglected.] The values of q_ω and Φ_ω at the actual interfaces $x=\pm L/2$ are found from the boundary conditions Eqs. (2.17) and (2.18). First note that while q_ω can be arbitrarily large on the electrode side, $\lambda_e q_\omega$ should remain finite, since it is equal to the total interface charge in the electrode. In the case when the screening length in the electrodes λ_e is much shorter than λ, Eq. (2.17) therefore gives (on the conductor side of the interface)

$$q_\omega\left(\pm\frac{L}{2}\right)=0. \tag{3.19}$$

Since the voltage drop in the electrode vanishes, the constraint of fixed voltage [i.e., the equivalent of Eq. (3.5)] in this model becomes

$$\Phi_\omega\left(\pm\frac{L}{2}\right)=\mp\frac{V_\omega A}{2}. \tag{3.20}$$

Integration of Eq. (3.18) from $\pm L/2$ to $\pm L'/2$, and use of Eq. (3.8) at $\pm L'/2$, now yields the required boundary conditions,

$$q_\omega\left(\pm\frac{L'}{2}\right)=\mp\frac{V_\omega A\sigma}{2D'}. \tag{3.21}$$

In this ground-plane model, finite charge densities in the conductor create image charges on the ground plane. Thus, at any finite frequency ω some parts of the interface currents are responsible for periodic recharging of the ground plane [see Fig. 1(c)]. Therefore, the current I^e_ω measured in the electrodes at a distance far from conductor-electrode interface may be different from the current which flows through this interface (note also that the two interface currents are not necessarily equal). In an experimental scheme symmetric with respect to the conductor, the current I^e_ω flowing into the external circuit is the symmetric component of the two currents:

$$I^e_\omega=\frac{1}{2}\left[I_\omega\left(-\frac{L}{2}\right)+I_\omega\left(\frac{L}{2}\right)\right]. \tag{3.22}$$

While the currents $I_\omega(\pm L/2)$ in this expression are the currents at the electrode side of the interfaces, due to Eq. (2.18) they are equal to $I_\omega(\pm L'/2)$. Of course, if the leads connecting the sample to the measurement instrument have some mutual capacitance, the current in the instrument will be less than $I^e(\omega)$ given by Eq. (3.22), but this loss factor may be taken into account by the standard circuit theory methods.

IV. THE RESPONSE FUNCTIONS

From now on we will consider the most natural case of well-conducting electrodes of size much larger than λ_e, and resistance negligible in comparison with the resistance $R=L/\sigma A$ of the conductor. We first show that the total noise produced in the electrodes is negligible compared to that originating in the conductor. For equilibrium noise, this is a direct consequence of the fluctuation-dissipation theorem. The same is true for shot noise, because of the fact that the electron distribution function in the electrodes is almost equilibrium. The electrode-conductor interface is also not an appreciable source of noise since, in the diffusion approximation studied here, the electron distribution at the conductor side of the interface is the same equilibrium Fermi distribution as in the electrode. Moreover, even deviations from

this approximation would result at the most in a few inelastic scattering events in the electrodes, leading to thermalization of hot electrons arriving from the conductor. As long as $l \ll L$, the number of those events per transferred electron is much smaller than the number of elastic events $[\sim(L/l)^2]$ the electron experiences in the conductor, so the thermalization process at the interface can also be neglected as a source of noise.

In this situation, the solutions to Eqs. (3.6) and (3.16) can thus be presented in the form

$$I_\omega(x)=Y(x;\omega)V_\omega+\frac{1}{L}\int_{-L/2}^{L/2}K(x,x';\omega)I_\omega^s(x')dx'. \tag{4.1}$$

Equation (4.1) shows that the current at frequency ω at any point x is composed of two components. The first is the response to the applied voltage across the conductor, and the second is the response to the random Langevin current sources inside the conductor.

The response functions $Y(x;\omega)$ and $K(x,x';\omega)$ are found by solving the equations for the current with $I_\omega^s(x)=0$ and $V_\omega=0$, respectively. They can be presented in a compact form by defining the following auxiliary functions, with $\eta=\kappa\lambda^2/\lambda_e$, $u=\kappa L/2$, $\mathrm{sinch}(u)=\sinh(u)/u$, $\Omega=\omega\epsilon/4\pi\sigma$, and $\chi=|x|-L/2$:

$$\mathcal{D}(\omega)=\frac{1}{\cosh(u)+\eta\,\sinh(u)}, \tag{4.2}$$

$$\mathcal{E}_\pm(x,\omega)=\begin{cases}\dfrac{u}{1-i\Omega}[\sinh(u\pm\kappa x)+\eta\,\cosh(u\pm\kappa x)] & (|x|<L/2),\\ \dfrac{u}{1-i\Omega}\,\eta\,\exp(-\kappa_e\chi) & (|x|>L/2),\end{cases} \tag{4.3}$$

$$\mathcal{F}(x,\omega)=\begin{cases}\dfrac{1-i\Omega\mathcal{D}(\omega)\cosh(\kappa x)}{[1-i\Omega][1-i\Omega\mathcal{D}(\omega)\mathrm{sinch}(u)]} & (|x|<L/2),\\ \dfrac{1-i\Omega[1-\eta\mathcal{D}(\omega)\sinh(u)\exp(-\kappa_e\chi)]}{[1-i\Omega][1-i\Omega\mathcal{D}(\omega)\mathrm{sinch}(u)]} & (|x|>L/2),\end{cases} \tag{4.4}$$

$$\mathcal{G}_\pm(x,\omega)=\frac{i\Omega\mathcal{E}_\pm(x,\omega)}{\sinh(u)+\eta\,\cosh(u)}, \tag{4.5}$$

$$\mathcal{H}_\pm(x,\omega)=i\Omega\mathcal{D}(\omega)[\mathcal{F}(x,\omega)+\mathcal{E}_\pm(x,\omega)]. \tag{4.6}$$

For the sandwich model, the response functions are

$$K(x,x';\omega)=\mathcal{F}(x,\omega)\pm\mathcal{G}_\pm(x,\omega)\sinh(\kappa x')-\mathcal{H}_\pm(x,\omega)\cosh(\kappa x') \tag{4.7}$$

and

$$Y(x;\omega)=\frac{1-i\Omega}{R}\mathcal{F}(x,\omega), \tag{4.8}$$

where, in Eq. (4.7), the upper sign should be used for $x'>x$ and the lower sign for $x'<x$.

In the ground-plane model, the functions K and Y inside the conductor are found to be the same as for the sandwich model (but with $D\to D'$) in the limit of vanishing conductivity of the conductor, i.e., in the formal limit $\eta^2\sim\Omega\to\infty$ (which also implies $\kappa=\overline{\kappa}$):

$$K(x,x';\omega)=\cosh(\overline{u}\pm\overline{\kappa}x)\frac{\cosh(\overline{u}+\overline{\kappa}x')}{\mathrm{sinch}(2\overline{u})} \tag{4.9}$$

with $\overline{u}=\overline{\kappa}L/2$ and with the upper sign used for $x'>x$ and the lower for $x'<x$. The response in the electrodes $K^e(x';\omega)$ to a fluctuation at x' is obtained with the help of Eq. (3.22),

$$K^e(x';\omega)=\frac{\cosh(\overline{\kappa}x')}{\mathrm{sinch}(\overline{u})}. \tag{4.10}$$

The response to voltage $Y(x,\omega)$ in this model is identical to $K^e(x;\omega)/R$,

$$Y(x;\omega)=\frac{1}{R}\frac{\cosh(\overline{\kappa}x)}{\mathrm{sinch}(\overline{u})}. \tag{4.11}$$

At low frequencies, and in both models, the response functions tend to constant values:

$$K(x,x';0)=1,\quad Y(x;0)=\frac{1}{R}. \tag{4.12}$$

Figure 3 shows the response functions for the sandwich model at intermediate and high frequencies. At $\omega\tau_T\gg1$, the responses are exponentially close to the source, i.e., to x' in the case of $K(x,x';\omega)$ and to $\pm L/2$ in the case of $Y(x;\omega)$. At any frequency and position, and for any value of L/λ,

$$\frac{1}{L}\int_{-L/2}^{L/2}K(x,x';\omega)dx'=1. \tag{4.13}$$

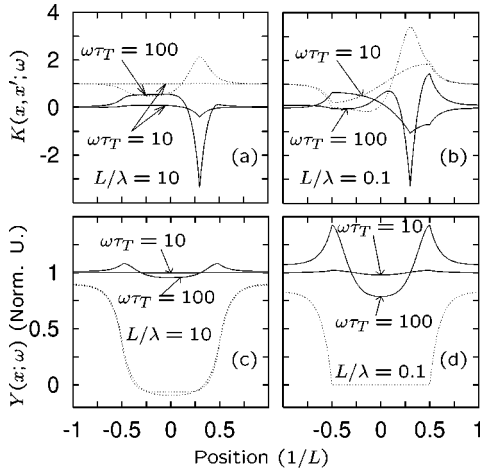

FIG. 3. Position dependence of the real (solid lines) and imaginary (dashed lines) parts of the response functions for the sandwich model at high frequencies, and for two values of L/λ. Re$[Y(x;\omega)]$ is in units of $1/R$. Im$[Y(x;\omega)]$ is in units of $-\Omega/R$. $x'=0.3$ here.

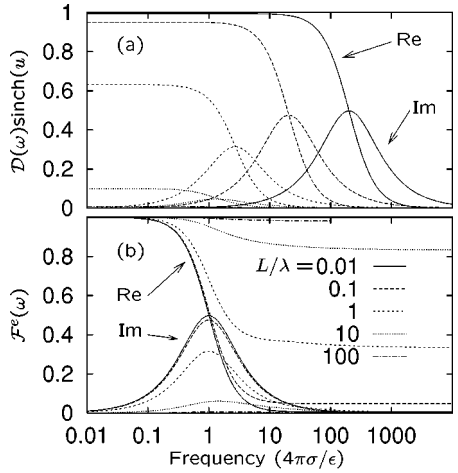

FIG. 4. The real and imaginary parts of the correction to the conductance of the sandwich model. The various curves are for different values of L/λ, and for $\lambda_e=\lambda$. (a) $\mathcal{D}(\omega)$sinch(u). The low-frequency value of this quantity is equal to one plus the emittance of the system. (b) $\mathcal{F}^e(\omega)=Y(\omega)/[(1-i\Omega)/R]$.

This general result is a manifestation of the constraint $V_\omega=0$, as can be seen by assuming a uniform current source in Eq. (4.1). Then, the only solution of the problem which maintains the constraint of fixed voltage is a uniform current everywhere, $I_\omega(x)=I^s_\omega$, leading immediately to Eq. (4.13).

The relation between the spectral density of the current noise $S_I(x,\omega)$ and the response function $K(x,x';\omega)$ is made clear through the identity

$$S_I(x,\omega)\,\delta(\omega)=2\langle I_\omega(x)I^*_\omega(x)\rangle. \tag{4.14}$$

With Eq. (4.1), and using the condition of fixed voltage and the locality of the current correlator [Eq. (2.14)], this expression becomes

$$S_I(x,\omega)=\frac{2A}{L^2}\int_{-L/2}^{L/2}|K(x,x';\omega)|^2\mathcal{S}(x')dx'. \tag{4.15}$$

The noise power deep inside the electrodes is given by

$$S_I(\omega)\equiv S_I(\infty,\omega). \tag{4.16}$$

The dynamic conductance is the response in the electrodes to external voltage,

$$Y(\omega)\equiv Y(\infty,\omega). \tag{4.17}$$

V. RESULTS: CONDUCTANCE AND EQUILIBRIUM NOISE

A. Sandwich model

For the sandwich model we have from Eqs. (4.4), (4.8), and (4.17)

$$Y(\omega)=\frac{1-i\Omega}{R}\,\frac{1}{1-i\Omega\mathcal{D}(\omega)\text{sinch}(u)}. \tag{5.1}$$

If the screening length in the electrodes is very small compared to L, then $\eta u\gg 1$, and we get

$$Y(\omega)=\frac{1-i\Omega}{R}=R^{-1}-i\omega C,\quad C=\frac{\epsilon A}{4\pi L}, \tag{5.2}$$

for any frequency ω. Equation (5.2) allows a simple interpretation: $Y(\omega)$ is just the complex admittance of the conductance R^{-1} coupled in parallel to the capacitor C formed by the two electrodes.

However, already at $L/\lambda_e=10$ the correction

$$\mathcal{F}^e(\omega)=\frac{1}{1-i\Omega\mathcal{D}(\omega)\text{sinch}(u)} \tag{5.3}$$

to this simple result is significant. Figure 4 shows the real and imaginary parts of this correction for different values of L/λ, for the case $\lambda=\lambda_e$ (for example, the conductor and the electrodes are made of the same material, but the electrodes have much fewer impurities). For $L/\lambda_e>1$, the correction term is insensitive to an increase of λ, so the appropriate curves of Fig. 4 also correspond to the case of a low-density conductor between metal electrodes. Figure 4(a) shows the term $\mathcal{D}(\omega)$sinch(u) which appears in the denominator of Eq. (5.1). The low-frequency value of this term is equal to $1-(4\pi\sigma/\epsilon)RE(0)$, with $E(0)\equiv i dY/d\omega|_{\omega=0}$ being the ''emittance.'' For a long conductor $(L/\lambda\gg 1)$

$$E(0)=\frac{\epsilon A}{4\pi L}=C. \tag{5.4}$$

As in Eq. (5.2), the emittance in this case can be viewed as the sum of the intrinsic emittance of the conductor and that of the capacitor formed by the electrodes. Then, the total emittance (5.4) is entirely due to the parallel-plate capacitance, and the emittance of the ''conductor itself'' equals zero, in agreement with the result of Ref. 21. However, as seen from Fig. 4(a), this result does not hold for a relatively short conductor, which means that the simple view of an additive emittance does not generally hold.

It is important to note that the calculations leading to Eq. (5.1) were not dependent on the distribution function of the electrons. Therefore, the correction to $Y(\omega)$ is due only to the screening properties of the system, and does not depend on thermalization or phase breaking of the electrons. Equation (5.1) is thus also valid if the inelastic scattering length is

smaller than L. Despite its mesoscopic nature [i.e., the fact that $Y(\omega)$ assumes its ordinary value Eq. (5.2) for large enough L], the correction discussed here should not be confused with other mesoscopic corrections to the conductivity of diffusive wires.[33]

Let us now comment on the possibility of observing the results depicted in Fig. 4. These results deviate from the standard theory only when L is comparable to λ and the frequency is comparable to the crossover frequency $2\sigma/\epsilon$. In order for the diffusion approximation used in Sec. II to apply to this regime, two conditions must be met:

$$k_F l \gg 2\pi \tag{5.5}$$

and

$$\frac{4\pi}{\epsilon}\sigma\tau = \frac{4k_F l^2}{3\pi a_0} \ll 1 \tag{5.6}$$

with $a_0 = \epsilon\hbar^2/me^2$ the effective Bohr radius. Combining the two leads to the condition[34]

$$k_F a_0 \gg \frac{16\pi}{3}. \tag{5.7}$$

The screening length λ is given by

$$\lambda = \left[\frac{\epsilon}{4\pi e^2 \mathcal{N}}\right]^{1/2} = \frac{1}{2}\left(\frac{\pi}{3}\right)^{1/6} a_0 (a_0 n^{1/3})^{-1/2}. \tag{5.8}$$

Combining Eqs. (5.7) and (5.8), we get the final criterion [in addition to Eq. (5.5)] which should be met in order to observe the results presented in this section:

$$a_0 \gg 5\lambda. \tag{5.9}$$

For example, in n-GaAs, $a_0 \approx 10$ nm, while in n-InSb, $a_0 \approx 60$ nm. Therefore, samples with $L/\lambda \sim 10$ (where we predict deviations of conductance by more than 15% from the results of the standard theory) can be implemented with no fundamental difficulties. As an example consider an InSb sandwich layer of thickness $L = 60$ nm with $n = 8\times 10^{19}$ cm^{-3} and $l = 8$ nm. Then $\lambda \approx 6$ nm, $\lambda_F \approx 4.7$ nm, $\sigma \approx 10^{15}$ Hz, and $\tau \approx 0.7$ fs, so that the required length hierarchy $L \gg l \gg \lambda_F$, as well as Eq. (5.6), are crudely achieved.[36] A practical realization of such an experiment might prove to be difficult, though, because of the high measurement frequencies involved (well in the optical range).

In order to implement, say, $L/\lambda \sim 0.1$, the thickness of an InSb layer should be smaller than 1 nm, i.e., a few atomic layers, so that our continuous model is at the border of its validity. Moreover, in the case $L \ll \lambda$, our model is strictly valid only if the scatterers in the dirty conductor are neutral (e.g., dipole scatterers). This is because the Coulombic potential of charged impurities would not be screened in this case and therefore the scattering would not be short-ranged, as assumed in Sec. II.

To summarize, the implementation of the ratio $L/\lambda \sim 1$ in the sandwich geometry seems possible in some special material systems. For lower ratios our continuous model is hardly adequate, at least for the materials we are aware of. For this reason, we will not discuss the sandwich model in the concluding Sec. VII (note that the above discussion does not apply to the ground-plane model). We have extended Fig. 4 to lower values of L/λ only to provide a better understanding of the effects of screening on the conductance of this conceptually simple system.

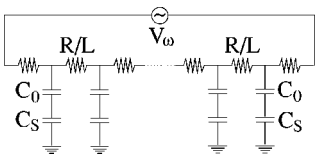

FIG. 5. Equivalent circuit for the geometry of the ground-plane model.

B. Ground-plane model

For the ground-plane model, Eqs. (3.22) and (4.11) lead to the following expression for the conductance of the system:

$$Y(\omega) = \frac{1}{R}\left(\frac{L}{\kappa\frac{L}{2}}\right)\mathrm{cth}\left(\frac{L}{\kappa\frac{L}{2}}\right). \tag{5.10}$$

This expression is identical to the conductance of a macroscopic wire of resistance R coupled to the ground plane via capacitance per unit length of

$$C_{\mathrm{eff}} = \left(\frac{1}{C_0} + \frac{1}{C_S}\right)^{-1}, \tag{5.11}$$

with

$$C_S = \frac{\epsilon A}{4\pi\lambda^2}. \tag{5.12}$$

The boundary conditions for this model, Eq. (3.21), can also be rewritten in terms of C_{eff} as

$$q_\omega\left(\pm\frac{L'}{2}\right) = \frac{V_\omega}{2} C_{\mathrm{eff}}. \tag{5.13}$$

Thus, the ground-plane model can be described by the equivalent circuit shown in Fig. 5. The capacitance C_S is due to the fact that in thin enough wires the screening is not efficient, so the current is determined by the gradient of the full electrochemical potential $\varphi = \Phi + A\mu/e$, rather than by $\Phi = Aq_\omega/C_0$ alone. In other words, additional charging of the wire increases not only its electrostatic energy ($\propto C_0^{-1}$), but also its internal energy ($\propto C_S^{-1}$), because of the necessary rise in the Fermi level. In 2D conductors, Eq. (5.12) reduces to the well-known result[37] for the two-dimensional electron gas. The effects of ''electrochemical capacitances'' similar to C_S on the emittance of ballistic structures were studied in Ref. 19. There is also a very interesting analogy between Eq. (5.12) and the expression $L_0^{-1} = A/4\pi\lambda^2$ (Ref. 38) for the specific kinetic inductance of a superconductor (in this case λ is London's penetration depth).

When $C_s \ll C_0$, the high-frequency ($\omega\overline{\tau}_T \gg 1$) conductance is given by

$$Y(\omega) = \frac{1}{R}\frac{L}{2\sqrt{iD/\omega}}, \tag{5.14}$$

the absolute value of which is just the dc conductance of a conductor of the same conductivity σ, but with length equal to twice the diffusion distance in time $1/\omega$. Thus, carriers injected at each of the electrodes are diffusing in and out of the conductor, without reaching the opposite electrode, and without affecting it by electric fields (the suppression of the longitudinal electric fields is the only role of the ground plane in this limit).

C. Equilibrium noise—Both models

Equilibrium thermal noise is related to the conductance by the fluctuation-dissipation theorem (we assume $T \gg \hbar\omega$)

$$S_I^{\rm eq}(\omega) = 4T\ {\rm Re}[Y(\omega)]. \tag{5.15}$$

However, since $Y(x,\omega)$ gives the current response to the *external* voltage, the local noise $S_I^{\rm eq}(x,\omega)$ is not directly related to it, and must be calculated independently.

At zero voltage, the average distribution function in the conductor is the Fermi-Dirac distribution given by Eq. (2.16). Using this distribution in Eq. (2.15) gives

$$\mathcal{S} = 2\sigma T \tag{5.16}$$

for the correlator of the Langevin sources. The spectral density for the equilibrium noise is thus found from Eq. (4.15),

$$S_I^{\rm eq}(x,\omega) = \frac{4T}{RL}\int_{-L/2}^{L/2} |K(x,x';\omega)|^2 dx'; \tag{5.17}$$

this equation in fact expresses the fluctuation-dissipation theorem for both the local and external fluctuations.

At zero frequency Eq. (4.12) gives

$$S_I^{\rm eq}(x,0) = \frac{4T}{R}, \tag{5.18}$$

as expected. At high frequencies ($\Omega, \omega\overline{\tau}_T \gg 1$), the equilibrium noise inside the conductor is given by

$$S_I^{\rm eq}(x,\omega) = \frac{2T}{R}\sqrt{\omega\overline{\tau}_T/2}\,[f(x)+f(-x)] \quad (|x|<L/2) \tag{5.19}$$

with

$$f(x) = 2e^{-\kappa_1 L}|\cosh(u-\kappa x)|^2[e^{2\kappa_1 x} - e^{-\kappa_1 L}] \tag{5.20}$$

and with $\kappa_1 = {\rm Re}(\kappa)$, so $\kappa_1 L = \sqrt{\omega\overline{\tau}_T/2}$. $f(x) = 1/2$ throughout the conductor, except at a narrow layer of width $1/\kappa_1$ near the edges, where it approaches its limiting values $f(-L/2) = 0$, $f(L/2) = 2$. The position and frequency dependence of $S_I^{\rm eq}$ is shown in Fig. 6(a) for the case $L/\lambda = L/\lambda_e = 10$. The general features here do not depend on screening.

The method presented here for calculating the conductance does not depend on the form of the distribution function [other than the diffusion approximation, Eq. (2.1)]. Therefore the results apply also to the case when strong ($l_{\rm ee} \ll L$, with $l_{\rm ee}$ the electron-electron scattering length) electron-electron scattering is present in the conductor. The equilibrium noise is also not affected by the e-e processes since this scattering does not affect the equilibrium Fermi-Dirac distribution, which is the input in Eq. (2.15).

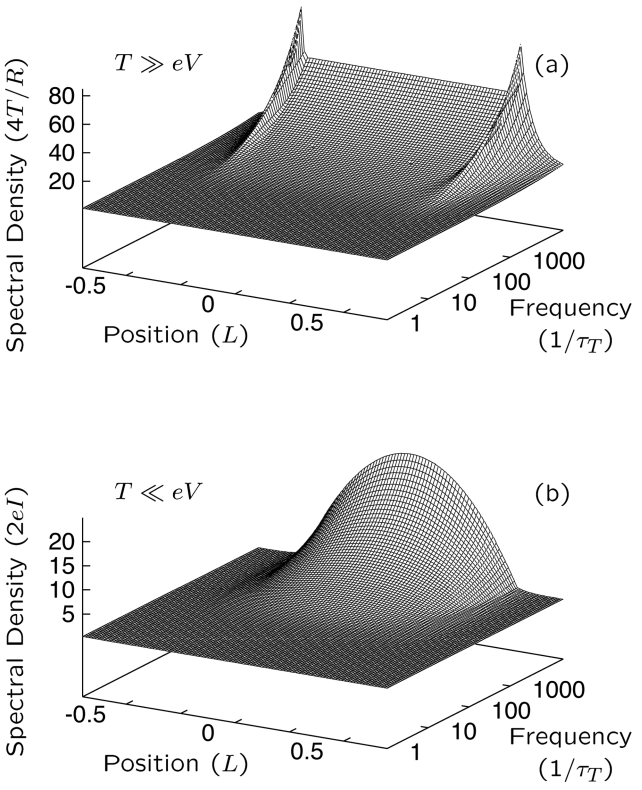

FIG. 6. Position and frequency dependence of the current noise intensity inside the conductor. (a) Equilibrium noise. (b) Shot noise. Here $L/\lambda = L/\lambda_e = 10$, but the general features of this figure are not sensitive to the screening properties.

VI. RESULTS: NONEQUILIBRIUM NOISE

In this section we will present the results on nonequilibrium noise for the ground-plane model; these results are also applicable for the sandwich model in the regime $\lambda, \lambda_e \gg L$. In the opposite limit ($\lambda, \lambda_e \ll L$) the noise in the sandwich model is white and is equal to the zero-frequency noise in the ground-plane model.[13] In contrast to the case of equilibrium noise, the shot noise is very sensitive to the strength of electron-electron interaction in the conductor, so we analyze this noise in the two limits of weak and strong e-e scattering.

A. Weak electron-electron scattering ($L \ll l_{\rm ee}$)

When $L \ll l_{\rm ee}$, the electron distribution function is found as a steady-state solution of Eq. (2.6). Under the condition (2.12) and for current perpendicular to the interfaces, it reads[3]

$$\overline{f_s}(E,x) = \left(\frac{1}{2}+\frac{x}{L}\right) f_0\left(E+\frac{1}{2}eV\right) + \left(\frac{1}{2}-\frac{x}{L}\right) f_0\left(E-\frac{1}{2}eV\right). \tag{6.1}$$

Equation (4.15) together with Eqs. (2.15) and (2.16) now give a general expression for the nonequilibrium noise,

$$S_I(x,\omega) = \frac{2}{RL}\int_{-L/2}^{L/2} dx' |K(x,x';\omega)|^2 \left[\mathcal{S}_+ + \mathcal{S}_- \frac{4x'^2}{L^2}\right] \tag{6.2}$$

with

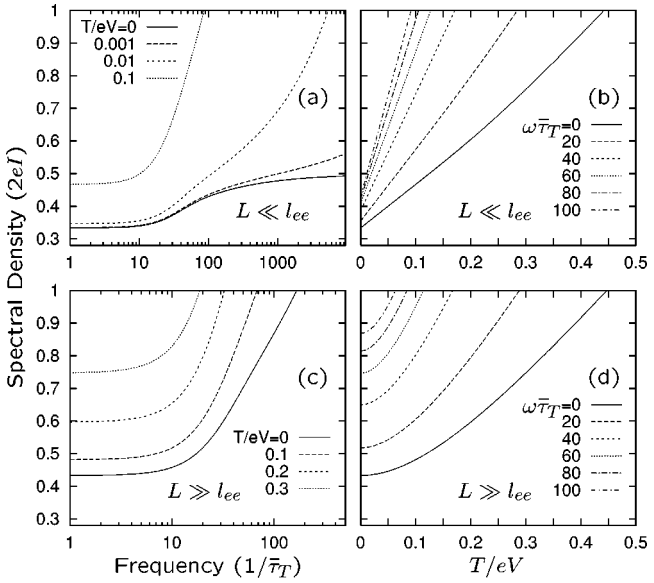

FIG. 7. Frequency and temperature dependence of the spectral density of the nonequilibrium noise in the limits of weak (a),(b) and strong (c),(d) electron-electron scattering.

$$\mathcal{S}_{\pm}(T,V)=T\pm\frac{eV}{2}\,\mathrm{cth}\left(\frac{eV}{2T}\right). \tag{6.3}$$

Figure 6(b) shows the spatial and frequency dependence of the shot noise for the case $L\gg\lambda,\lambda_e$ and $T\ll eV$. It is remarkable that inside the conductor the high-frequency noise is large even at zero temperature:

$$S_I(x,\omega)=\frac{eI}{2}\sqrt{\frac{\omega\bar{\tau}_T}{2}}\left(1-\frac{4x^2}{L^2}\right)\quad(\omega\bar{\tau}_T\gg 1). \tag{6.4}$$

This rise is due to the highly nonequilibrium distribution of carriers, Eq. (6.1). Specifically, at any frequency ω the current fluctuations at position x are due only to electrons at distances $\sim\sqrt{D/\omega}$ from x. The smaller this range, the smaller is the smoothing of the singularity in the energy distribution of the electrons in the range, and the larger is the noise.

The noise in the external electrodes is found by using the external response function $K^e(x';\omega)$ in Eq. (6.2). Whenever $K^e(x';\omega)=1$, i.e., at low frequencies, or when $\lambda,\lambda_e\ll L$ in the sandwich model, Eq. (6.2) reduces to

$$S_I(\omega)=\frac{4}{R}\left[\frac{2}{3}T+\frac{1}{6}eV\,\mathrm{cth}\left(\frac{eV}{2T}\right)\right] \tag{6.5}$$

as was found by Nagaev.[3] However, in the general case, the noise in the electrodes exhibits strong frequency dependence on a frequency scale of the order of the inverse effective Thouless time $1/\bar{\tau}_T$, which is also affected by the screening lengths λ,λ_e.[13] Figures 7(a) and 7(b) show the dependence of the noise on frequency and temperature in the ground-plane model. At $\omega\bar{\tau}_T\gg 1$,

$$S_I(\omega)=\frac{2T}{R}(\sqrt{\omega\bar{\tau}_T/2}-1)+eI\,\mathrm{cth}\left(\frac{eV}{2T}\right)+O\left(\frac{1}{\sqrt{\omega}}\right). \tag{6.6}$$

At strictly zero temperature, Eq. (6.6) gives the high-frequency result presented in (Ref. 13):

$$S_I(\omega)=eI. \tag{6.7}$$

At finite temperatures, an additional crossover appears at $\omega\bar{\tau}_T\sim(eV/T)^2/2$, above which the equilibrium noise dominates [Fig. 7(a)]. At any frequency, Eq. (6.6) shows that noise grows *linearly* with the temperature, Fig. 7(b).

The frequency dependence of the zero-temperature noise in the conductor is the same as that of the finite-temperature noise [compare Eq. (6.6) with Eq. (6.4)]. Therefore, one can assign an effective position-dependent temperature to the distribution function (6.1):

$$T_{\mathrm{eff}}(x)=\frac{eV}{4}\left(1-\frac{4x^2}{L^2}\right). \tag{6.8}$$

Note, however, that this distribution function does not have the Fermi-Dirac form.

B. Strong electron-electron scattering ($L\gg l_{ee}$)

We now consider the case when electron-electron scattering is so strong that the scattering length l_{ee} is much smaller than L (though still larger than l), but is weak enough so the single-particle Boltzmann equation is still valid ($l_{ee}\gg\lambda_F$). Its solution is then given by the local-equilibrium distribution

$$f(E,x)=\frac{1}{1+\exp\left[\dfrac{E-\mu(x)}{T_e(x)}\right]} \tag{6.9}$$

with

$$\mu(x)=\mu-\frac{x}{L}eV \tag{6.10}$$

and with a local electron temperature T_e which satisfies the equation[9,10]

$$\frac{d^2}{dx^2}T_e^2(x)=-\frac{6(eV)^2}{\pi^2L^2} \tag{6.11}$$

under the boundary conditions $T_e=T$ at $x=\pm L/2$. The electron temperature is thus given by

$$T_e(x)=T\sqrt{1+\xi^2[1-(2x/L)^2]} \tag{6.12}$$

with

$$\xi=\frac{\sqrt{3}eV}{2\pi T}. \tag{6.13}$$

This distribution was also found in Ref. 5 by separating the conductor into coupled phase-coherent conductors of length l_{ee}.

With this distribution, the current correlator (2.15) becomes

$$\mathcal{S}(x)=2\sigma T_e(x) \tag{6.14}$$

so the nonequilibrium noise in the system is

$$S_I(x,\omega)=\frac{4}{RL}\int_{-L/2}^{L/2}dx'|K(x,x';\omega)|^2T_e(x'). \quad (6.15)$$

In what follows, we will concentrate on the current noise present in the electrodes. In all cases for which $K^e(x';\omega)=1$ (i.e., $\omega\bar{\tau}_T\ll 1$ or $L\gg\lambda,\lambda_e$ in the sandwich model), the result obtained in Ref. 5 is recovered:

$$S_I(\omega)=\frac{2T}{R}\left[1+\left(\xi+\frac{1}{\xi}\right)\arctan(\xi)\right]. \quad (6.16)$$

At high temperatures ($\xi\ll 1$), Eq. (6.16) gives the regular equilibrium noise $S_I(\omega)=4T/R$. At low temperatures the well-known result[5,9,10]

$$S_I(\omega)=\frac{\sqrt{3}eI}{2} \quad (6.17)$$

is obtained.

All the above results are very close to those for $L\ll l_{ee}$. However, the *high-frequency* behavior of nonequilibrium noise in a system with $L\gg l_{ee}$ is radically different from that in a system with $L\ll l_{ee}$.

Figures 7(c) and 7(d) show the spectral density $S_I(\omega)$ as a function of frequency and temperature for the ground-plane model (or, equivalently, the sandwich model with $L\ll\lambda,\lambda_e$), with the response function (4.10). In the high-frequency limit, Eq. (6.15) yields

$$S_I(\omega)=\frac{T}{R}\omega\bar{\tau}_T\int_0^1 e^{\kappa_1 L(y-1)}\sqrt{1+\xi^2(1-y^2)}dy. \quad (6.18)$$

The characteristic parameter of this integral is the ratio

$$\xi_0=\frac{2\xi^2}{\sqrt{\omega\bar{\tau}_T/2}}=\frac{3(eV)^2}{2\pi^2T^2\sqrt{\omega\bar{\tau}_T/2}}. \quad (6.19)$$

At small and large values of this ratio, Eq. (6.18) gives, respectively,

$$S_I(\omega)=\frac{2T}{R}\left(\frac{\omega\bar{\tau}_T}{2}\right)^{1/2}+\frac{3R(eI)^2}{2\pi^2T} \quad [eV\ll T(\omega\bar{\tau}_T)^{1/4}], \quad (6.20a)$$

$$S_I(\omega)=\sqrt{\frac{2\pi^3}{3}}\left(\frac{\omega\bar{\tau}_T}{2}\right)^{3/4}\frac{T^2}{R^2eI}+\sqrt{\frac{3}{2\pi}}\left(\frac{\omega\bar{\tau}_T}{2}\right)^{1/4}I \quad [eV\gg T(\omega\bar{\tau}_T)^{1/4}]. \quad (6.20b)$$

At high temperatures Eq. (6.20a) is always valid. The leading term in $\omega\bar{\tau}_T$ is the same as for $L\ll l_{ee}$. However, in contrast to Eq. (6.6), the nonequilibrium correction to this noise has a *quadratic* dependence on the current I.

More interesting is the low-temperature limit, $\xi\gg 1$. As long as the frequency is not very high, $\xi_0>1$, the nonequilibrium term is linear in eI, as usual. However, even at $T\to 0$ the noise grows with ω indefinitely as $(\omega\bar{\tau}_T)^{1/4}$ [as opposed to the case of $l_{ee}\gg L$, see Eq. (6.7)]. This dependence and the transition to $\omega^{1/2}$ dependence at high enough temperature or frequency are shown in Fig. 7(c). The low-temperature behavior of the high-frequency noise can be understood by comparing the noise correlators $\mathcal{S}$ in Eqs. (6.2) and (6.14): The response function $K^e(x';\omega)$ [Eq. (4.10)] is significant only for sources at x' within a distance $\sqrt{D'/\omega}$ from the interfaces with the electrodes. Therefore, the correlator (6.14), which drops more gradually near $x=\pm L/2$ than the correlator in Eq. (6.2), produces noise in the electrodes, which grows faster with frequency.

The transition to thermal noise at low temperature now occurs at $\omega\bar{\tau}_T\sim(eV/T)^4/20$ (i.e., at higher frequencies than for the case $l_{ee}\gg L$). Below this crossover Eq. (6.20b) is valid, and the thermal term is now *quadratic* in T, Fig. 7(d). These two results, namely, the unbound increase of the noise with frequency at $T=0$ and the T^2 correction to the shot noise, are unique to systems with strong e-e interaction, and can serve as a clear experimental identification of such interactions.

VII. DISCUSSION AND CONCLUSIONS

We believe that our work has produced two major results of general importance. First, the high-frequency noise of small diffusive conductors is considerably affected by screening in the conductor, the electrodes leading to the conductor, and the surrounding media. Screening also has a measurable effect on the ac conductance of the system. The ''external screening'' is in fact an intrinsic part of the problem. For example, the effects of screening on the dynamic properties are very different for our two model geometries, which basically differ only in their external electromagnetic environment.

In particular, with due account of screening, the noise spectrum is *not* white even at frequencies for which quantum fluctuations are negligible and the Drude conductance is frequency-independent (i.e., $\omega\ll eV/\hbar,1/\tau$). This result is due to the fact that at frequencies higher than the inverse Thouless time, the current in the electrodes may be responding only to fluctuations in the conductor which are within a distance $1/\bar{\kappa}\ll L$ from the interfaces with the electrodes [see Eq. (4.10)]. In these regions the distribution function is nearly equilibrium, and therefore the noise is strongly suppressed: its effective temperature (at $T=0$) is $eV/\bar{\kappa}L$, Eq. (6.8). However, in order to satisfy the basic relation (4.13), the external response to fluctuations in those regions must be very large, $K^e(x';\omega)=\bar{\kappa}L/2$ [see also Eq. (4.10)]. Thus, each interface can be viewed as a fundamental noise source of temperature $eV/2$, which is just the effective temperature of the classical Schottky noise. Since the two sources are not correlated, the total noise in the electrode is 1/2 of the Schottky value, Eq. (6.7). [In the sandwich model, the above description holds only for the case $L\ll\lambda,\lambda_e$. In the opposite limit, the strong screening allows the current in the electrodes to respond uniformly to all fluctuations in the conductor, thus retaining the 1/3 suppression factor, Eq. (6.5)].

The reason for the peculiarity of the ground-plane model is now apparent. Here, charge fluctuations in the conductor are screened by the close ground plane. Therefore, high-frequency fluctuations inside the conductor are not felt by the electrodes even if screening is strong in the conductor and

the electrodes. Thus, the frequency dispersion of the noise is obtained in this model even if $\lambda, \lambda_e \ll L$.

Notice that the result (3.22), and therefore Eq. (6.7), is exactly valid only for the case in which the voltage drop, and the ground plane, are symmetric with respect to the length of the conductor. If, for instance, the ground plane is coupled much more strongly to the right electrode, then the current through the electrodes would be the same as the current at the left conductor-electrode interface, and the noise value would be $2eI$. Thus, Eq. (6.7) is not universal in the sense that by changing the geometry of the system any noise value between eI and $2eI$ can be obtained.

The effect of screening on noise discussed in this work is very different from the effect it has on classical shot noise in vacuum diodes. In the latter case,[11] the low-frequency noise is suppressed when the space-charge in the diode (and thus the screening) is large. This is due to the fact that, say, an upward instantaneous fluctuation of electron emission results in an increase of negative space charge and hence the potential barrier near the emitter, so that not all excess electrons arrive at the collector. Since the thermionic current depends exponentially on the barrier height, this negative feedback is very effective, and the shot noise may be considerably lower than the Schottky value. In our case, however, this is not true. Since the Fermi level is higher than the electrostatic potential, electron potential fluctuations throughout the device hardly affect the current.

Our second major result is that the high-frequency noise in diffusive conductors is strongly dependent upon the strength of the short-range electron-electron scattering. When such scattering is strong, the nonequilibrium noise is not only nonwhite, but does not even saturate at high frequencies, and can in fact be larger than the classical noise value $2eI$. The quadratic dependence of the noise on temperature for this case, as opposed to the linear dependence in the case of weak e-e scattering (see Fig. 7), indicates that the sources of the two types of noise, namely the thermal and shot noise, are coupled when $L \gg l_{ee}$, but are independent (and thus additive) in the opposite limit, $L \ll l_{ee}$. In addition to the basic significance of this result, the different functional dependence can serve as an experimental diagnostic tool for the determination of the ratio $\beta = L/l_{ee}$ in a given sample. Other quantities which are sensitive to this ratio are usually due to phase coherence of the electrons (and its absence at $\beta \gg 1$) such as the corrections to the conductance due to weak localization[22] (as noted above, the regular, semiclassical conductance is not sensitive to e-e scattering). In our case, however, the strong dependence on β is purely semiclassical, as it is due to the difference between the distribution functions at different values of β.

The large value of noise at high frequencies is due to the forms of the nonequilibrium distribution function and the response function, as was explained in Sec. VI B. Ultimately, it originates from screening which relates the measured current fluctuations in the electrodes to the scattering of *many* electrons in the conductor, all behaving collectively. Thus, it should not be too surprising that at some particular situations correlations are such that the measured noise is larger than the single-particle classical shot noise value $2eI$. The same is true for the increase of noise with frequency, which is quite different from the usual behavior of high-frequency noise. For example, regular ''diffusion noise'' in semiconductors (see, e.g., Ref. 28) *decreases* with frequency with the same characteristic frequency $1/\tau_T$ as in the present work. However, this type of noise is very different from the one studied here: classical diffusion noise is modulation noise, i.e., noise due to the change in the conductance when electrons are diffusing in and out of the sample. It is a second-order effect proportional to I^2, unlike the shot noise which is proportional to I. Our arguments show [see Eqs. (2.9) and (2.12)] that modulation noise is negligible in the degenerate system we are studying if the density fluctuations are much smaller than the average electron density. This condition is clearly fulfilled in our system.

Generally, in any semiclassical theory noise must eventually decrease with frequency. In our case, this happens at frequencies higher than the inverse elastic scattering time $1/\tau$, as can be concluded from Eq. (2.4b): at $\omega \gg 1/\tau$ fluctuations of f_a, and thus of the current, are proportional to $1/\omega$ [in this limit the Langevin source to be added to Eq. (2.4b) would also depend on frequency, since the scattering events are correlated at times shorter than τ]. At $\omega \ll 1/\tau$, however, it is only f_s (i.e., the density), and not f_a, which is directly dependent on frequency [see Eqs. (2.4)]. The reason why this dependence does not necessarily imply a decrease of the current fluctuations with frequency is evident from the simple discussion of Sec. III A.

In recent years there has been a growing experimental interest in the dynamic properties of diffusive mesoscopic structures. While the results presented here are consistent with the results of all the relevant published experiments of which we are aware, none of those experiments explore the regions where we predict deviations from previous theories. The ac conductance of diffusive samples was measured at microwave frequencies with the motivation of comparison with weak localization theories.[23,39,40] Thus, in all those experiments the samples were very much longer than the screening length, and a ground plane was not available. Noise measurements also did not reach the frequency range of interest. In Refs. 41–43, the observation frequencies were 400 KHz (or less). In Ref. 44, the noise was measured at frequencies up to 20 GHz, but the sample was made of relatively well-conducting gold, with an inverse Thouless time of about 100 GHz. Nevertheless, we see that the experimental parameters are quite close to those studied in this work.

Due to the reasons discussed in the end of Sec. V A, it seems that the experimental verification of the results presented in this work should be mainly feasible using thin conductors located very close to a ground plane (gate). In many experiments this geometry is a natural choice (e.g., when the conductor is two-dimensional), due to its simple fabrication procedure. This geometry also presents the possibility of controlling the conductor's parameters with gate voltage, cf. Ref. 41. For typical experimental parameters,[41] $D' \sim D \sim 10^3$ cm^2/s and $L \sim 10$ μm, the expected crossover frequency in this geometry is $30/2\pi\overline{\tau}_T \sim 5$ GHz, i.e., within the range currently available for accurate noise measurements (cf. Refs. 44 and 45).

Compared to the measurements of the noise in the electrodes, measurements of the local noise [Figs. 6(a) and 6(b)] seem much more difficult. Nevertheless, one can think of novel techniques to measure this quantity. For instance, a

measurement scheme of the local potential spectral density, which is directly related to $S_I(x,\omega)$ by the continuity equation, can be made possible by means of a capacitative coupling of some point in the conductor to an external single-electron-transistor probe.[46] The observation of this noise is then facilitated by its very large magnitude (Fig. 6).

ACKNOWLEDGMENTS

Discussions with M. Buttiker, A. N. Korotkov, B. Laikhtman, R. Landauer, Z. Ovadyahu, and R. J. Schoelkopf are gratefully acknowledged. The work was supported in part by DOE's Grant No. DE-FG02-95ER14575.

[1] D. V. Averin and K. K. Likharev, in *Mesoscopic Phenomena in Solids*, edited by B. L. Altshuler, P. A. Lee, and R. A. Webb (Elsevier, Amsterdam, 1991).
[2] C. W. J. Beenakker and M. Büttiker, Phys. Rev. B **46**, 1889 (1992).
[3] K. E. Nagaev, Phys. Lett. A **169**, 103 (1992).
[4] Yu. Nazarov, Phys. Rev. Lett. **73**, 134 (1994).
[5] M. J. M. de Jong and C. W. J. Beenakker, Physica A **230**, 219 (1996).
[6] Ya. M. Blanter and M. Büttiker, Phys. Rev. B **56**, 2127 (1997).
[7] M. J. M. de Jong and C. W. J. Beenakker, in *Coulomb and Interference Effects in Small Electronic Structures*, edited by D. C. Glattli and M. Sanquer (Editions Frontiéres, France, 1995).
[8] Other views consider the agreement between the two theories as a sheer coincidence: R. Landauer, Physica B **227**, 156 (1996); private communication.
[9] K. E. Nagaev, Phys. Rev. B **52**, 4740 (1995).
[10] V. I. Kozub and A. M. Rudin, Surf. Sci. **361/362**, 722 (1996).
[11] A. van der Ziel, *Noise* (Prentice-Hall, Englewood Cliffs, NJ, 1954).
[12] B. L. Altshuler, L. S. Levitov, and A. Yu. Yakovets, Pis'ma Zh. Éksp. Teor. Fiz. **59**, 821 (1994) [JETP Lett. **59**, 857 (1994)].
[13] Y. Naveh, D. V. Averin, and K. K. Likharev, Phys. Rev. Lett. **79**, 3482 (1997).
[14] Behavior of the noise at the electrode-conductor interface in a similar model was also calculated by K. E. Nagaev, Phys. Rev. B **57**, 4628 (1998).
[15] Y. Imry and N. S. Shiren, Phys. Rev. B **33**, 7992 (1986).
[16] M. Büttiker, Ann. (N.Y.) Acad. Sci. **480**, 195 (1986).
[17] Y. Gefen and O. Entin-Wohlman, Ann. Phys. (N.Y.) **206**, 68 (1991).
[18] B. Reulet and H. Bouchiat, Phys. Rev. B **50**, 2259 (1994).
[19] M. Büttiker, J. Phys.: Condens. Matter **5**, 9361 (1993).
[20] M. Büttiker, J. Math. Phys. **37**, 4793 (1996).
[21] M. Buttiker and T. Christen, in *Theory of Transport Properties of Semiconductor Nanostructures*, edited by E. Schöll (Chapman and Hall, London, 1998).
[22] B. L. Altshuler, A. G. Aronov, D. E. Khmelnitskii, and A. I. Larkin, in *Quantum Theory of Solids*, edited by I. M. Lifshits, Advances in Science and Technology in the USSR, Physics Series (Mir, Moscow, 1982).
[23] S. A. Vitkalov, Zh. Éksp. Teor. Fiz. **109**, 1846 (1996) [JETP **82**, 994 (1996)].
[24] P. W. Brouwer and M. Büttiker, Europhys. Lett. **37**, 441 (1997).
[25] F. von Oppen and A. Stern, Phys. Rev. Lett. **79**, 1114 (1997).
[26] That screening may affect the noise was first suggested by R. Landauer, Ann. (N.Y.) Acad. Sci. **755**, 417 (1995).
[27] Sh. M. Kogan and A. Ya. Shul'man, Zh. Éksp. Teor. Fiz. **56**, 862 (1969) [Sov. Phys. JETP **29**, 467 (1969)].
[28] Sh. Kogan, *Electronic Noise and Fluctuations in Solids* (Cambridge University Press, Cambridge, 1996), p. 80.
[29] E. M. Lifshitz and L. P. Pitaevskii, *Physical Kinetics* (Pergamon, Oxford, 1981), Sec. 83.
[30] The reader is reminded that ρ is the *excess* charge density, i.e., $\rho=\int d\varepsilon\, g(\varepsilon)(f_s-\overline{f_s})$ with $g(\varepsilon)$ the density of states.
[31] In the case when the interfaces between the conductor and the electrodes are smooth on the scale of l, the diffusion approximation applies also to the interface region, and the boundary conditions (2.17) and (2.18) [as well as their detailed form, the continuity of $f_s(\varepsilon)$ and of $\varepsilon_{\mathbf{k}} f_a(\varepsilon)$] can be obtained directly by integrating Eq. (2.6) across the interface region.
[32] W. R. Smythe, *Static and Dynamic Electricity*, 3rd ed. (McGraw-Hill, New York, 1968), p. 78.
[33] Y. Imry, in *Direction in Condensed Matter Physics*, edited by G. Grinstein and G. Mazenko (World Scientific, Singapore, 1986).
[34] This condition is stronger than the Mott criterion (Ref. 35) $k_F a_0 > 0.8$ necessary for the electrons to be delocalized.
[35] R. F. Milligan, T. F. Rosenbaum, R. N. Bhatt, and G. A. Thomas, in *Electron-Electron Interactions in Disordered Systems*, edited by A. L. Efros and M. Pollak (North-Holland, Amsterdam, 1985).
[36] We have used $\epsilon=16.8$ and $m=0.0136m_e$ as the InSb parameters, *Landolt-Börnstein Numerical Data and Functional Relationships in Science and Technology*, Vol. 17a, edited by O. Madelung (Springer-Verlag, Berlin, 1982).
[37] S. Luryi, Appl. Phys. Lett. **52**, 501 (1988).
[38] See, e.g., K. Likharev, Radiophys. Quantum Electron. **14**, 964 (1972).
[39] J. B. Pieper, J. C. Price, and J. M. Martinis, Phys. Rev. B **45**, 3857 (1992).
[40] G. U. Sumanasekera, B. D. Williams, D. V. Baxter, and J. P. Carini, Solid State Commun. **85**, 941 (1993).
[41] F. Liefrink, J. I. Dijkhuis, M. J. M. de Jong, L. W. Molenkamp, and H. van Houten, Phys. Rev. B **49**, 14 066 (1994).
[42] A. H. Steinbach, J. M. Martinis, and M. H. Devoret, Phys. Rev. Lett. **76**, 3806 (1996).
[43] M. Henny, H. Birk, R. Huber, C. Strunk, A. Bachtold, M. Krüger, and C. Schönenberger, Appl. Phys. Lett. **71**, 773 (1997).
[44] R. J. Schoelkopf, P. J. Burke, A. Kozhevnikov, D. E. Prober, and M. J. Rooks, Phys. Rev. Lett. **78**, 3370 (1997).
[45] M. Reznikov, M. Heiblum, H. Shtrikman, and D. Mahalu, Phys. Rev. Lett. **75**, 3340 (1995).
[46] R. J. Schoelkopf (private communication).